

MOR-83-655

Technical Report
Contract N00014-83-C-0080

AD A137272

Effects of Yttrium Microalloying on the Epitaxial Grain Growth in Ti-6Al-4V Weld Fusion Zones

Mohan S. Misra
Martin Marietta Aerospace
P.O. Box 179
Denver, Colorado 80201

October 1983

Prepared for:

Office of Naval Research
800 N. Quince Street
Arlington, VA 22217

DTIC
ELECTRONIC

JAN 26 1984

A

This document has been approved
for public release and sale; its
distribution is unlimited.

83 11 15 031

BEST AVAILABLE COPY

Technical Report
Contract N00014-83-C-0090

Effects of Yttrium Microalloying on the Epitaxial Grain Growth in Ti-6Al-4V Weld Fusion Zones

Mohan S. Misra
Martin Marietta Aerospace
P.O. Box 179
Denver, Colorado 80201

October 1983

Prepared for:

Office of Naval Research
800 N. Quince Street
Arlington, VA 22217

FOREWORD

This technical report summarizes work performed from November 5, 1982 to August 4, 1983 under the Office of Naval Research (ONR) sponsored contract N00014-83-C-0090. Dr. B. MacDonald was the ONR scientific officer directing the program, which was carried out at Martin Marietta Denver Aerospace with Mr. Mohan S. Misra as the program manager and principal investigator.



Letter on file

Dist		Special	
A-1			

SUMMARY

→ The fusion zone microstructure in Ti-6Al-4V welds consists of long columnar grains, grown epitaxially from the fusion zone (FZ)/heat affected zone (HAZ) interface. Introducing small amounts (0.01 to 0.1 wt %) of yttrium to the fusion zone by microalloyed filler wire, results in significant grain refinement. However, initial grains still grow epitaxially, suggesting that some time dependent processes are responsible for the observed refinement away from the FZ/HAZ interface. Classical nucleation and growth theories were modified by introducing two competing time concepts; one time to nucleate one grain and the other time for epitaxial grains to grow across the total width of the bead.

The theoretical model was verified experimentally by determining the nucleation time and growth rate from the microstructural observation of grain orientation with respect to welding direction and speed. Yttrium microalloying increases the solidification rate and decreases the nucleation time. The later effect is more pronounced and is responsible for the fusion zone grain refinement. ←

INTRODUCTION

The initial weld pool solidification in aluminum¹ and iron base alloys² occurs by epitaxial grain growth at the fusion and heat-affected zone interface. The incompletely melted solid grains at the liquid-solid interface provide an ideal substrate on which continued growth can take place with a minimal amount of supercooling. In single pass welds of these alloys, the grain structure consists of initial epitaxial grains extending from the FZ/HAZ interface, followed by equiaxed grains. In multiple pass welds the same grain structure repeats from bead to bead. However, in Ti-6Al-4V alloy welds, epitaxial grains grow across the total width of the fusion zone and then continue to grow across the fusion lines during subsequent weld passes without nucleating new grains, resulting in extremely long columnar grains as shown in Figure 1. The grain boundaries so formed could provide a continuous crack path. Naturally one of the objectives in multiple pass titanium welds would be to prevent epitaxial growth and break up the coarse columnar fusion zone grain structure in the fusion zone.

There are many methods to refine the fusion zone grain structure including: (1) mechanical-electrical stirring of the weld pool; (2) modification of process parameters; and (3) addition of nucleation agents or inoculants. The recent application of pulsed arc to Ti-6Al-4V welds³ was not successful and the results of Brown et al.⁴ on the application of vibrational energy to weld metal solidification likewise were not very encouraging. Savage and Aronson⁵ theorized that the mechanical vibrations to refine the fusion zone grain size are likely to meet with failure because epitaxial solidification requires a minimum amount of supercooling and it is unlikely that sufficient supercooling can be induced by mechanical vibration to cause nucleation.



Intergranular Crack



Grain Boundary α
(Crack Along Interface)

Figure 1
Four pass GTA weld in Ti-6Al-4V alloy using Ti-6Al-4V filler wire. Shows long columnar grains in fusion zone. The crack follows grain boundary α .

The use of nucleating agents to refine the grain size in castings has been widely practiced. This includes titanium and boron in aluminum and zirconium and rare earths in magnesium. Similarly, nucleation effects of minor alloying element additions in pure metals and alloys have been studied by a number of researchers.^{6,7} However, very limited data is available regarding inoculant effects on the weld pool solidification, especially in titanium alloys. Glickenstein and Yeniscavich⁸ have reviewed minor element effects on the welding arc and weld penetration and it appears that these elements can also affect the solidification kinetics in the weld pool by influencing supercooling, surface tension, and fluid motion.

The work of Rath et al.⁹ indicated that small amounts of yttrium and erbium significantly retard the solid state recrystallization and grain growth kinetics in titanium alloys. Simpson¹⁰ demonstrated the effectiveness of yttrium on the fusion zone grain refinement in Ti-6Al-6V-2Sn welds; however, his work did not involve solidification kinetics or supercooling studies.

Preliminary work performed at Denver Aerospace and the Colorado School of Mines¹¹ has established that small amounts of yttrium, when added to the Ti-6Al-4V fusion zone, refines the grain structure and increases the weld penetration.

The objectives of this work were to (1) quantify the influence of yttrium microalloying on the fusion zone grain refinement; and (2) develop a nucleation and growth model to predict weld pool solidification microstructure, with and without microalloy additions.

EXPERIMENTAL PROCEDURE

Weld Preparation - All the welds were prepared by the Gas Tungsten Arc (GTA) process using the following process parameters:

- 1) Shield gas - helium:
 - a. Torch - 50 cubic feet per hour (CFH),
 - b. Trailer - 75 CFH,
 - c. Backup - 10 CFH;
- 2) Travel speed - 5 ipm (2.1 mm/s).

Travel speed was kept constant for all the welds. Heat input and yttrium concentrations were studied as process variables and are listed in Table 1 along with the specimen thickness.

Table 1 Process Variables

Weld Schedule	Plate Thickness	Number of Passes	Heat Input	Y Conc
A	0.500	15	C	N
B	0.875	22	V	N
C	0.500	15	C	V
D	0.875	20	V	V
E	0.875	18	V	V
F	0.160	1	C	N
G	0.160	1	C	C
V - Variable C - Constant N - Nil				

Heat input was varied by changing the current while keeping the voltage constant. A special Ti-6Al-4V filler wire with approximately 0.5 wt % Y was fabricated to introduce Y in the weld pool. Yttrium concentration was manipulated either by changing the wire feed rate or using a dual wire feed system with Ti-6Al-4V wire to dilute the Y concentration. The schedules for thick section welds are listed in Tables 2 through 8 and the filler wire fabrication is described in the following section.

Table 2 Weld Schedule A

Pass No.	V(v)	I(A)	Wire Speed (ipm)
1	9.0	140	20
2	9.0	136	25
3	9.0	136	30
4	9.5	136	30
5	9.5	136	30
6	9.5	136	30
7	9.5	136	30
8	9.5	136	30
9	9.5	136	30
10	9.5	135	30
11	9.5	140	30
12	9.5	140	30
13	9.5	140	30
14	9.5	140	30
15	9.5	140	30
Base Metal: Ti-6Al-4V, 0.50 in. Thick Plate Filler Metal: Ti-6Al-4V, 0.045 in. dia Helium Shield Gas: 50 CFH Torch, 75 CFH Trailer, 10 CFH Backup Torch Travel Speed, 5 ipm			

Table 3 Weld Schedule B

Pass No.	V(v)	I(A)	Wire Speed (ipm)
1	9.0	140	20
2	9.0	140	25
3	9.5	152	35
4	9.5	150	36
5	9.5	168	36
6	10.0	180	36
7	10.0	180	36
8	10.3	185	40
9	10.5	187	40
10	10.5	190	45
11	10.5	195	45
12	10.5	195	45
13	10.5	195	45
14	10.5	195	45
15	10.5	195	45
16	10.5	195	45
17	10.5	200	45
18	10.5	200	50
19	10.5	200	50
20	10.5	200	50
21	10.5	200	50
22	10.5	200	50
Base Metal: Ti-6Al-4V, 0.875 in. Thick Plate Filler Metal: Ti-6Al-4V, 0.045 in. dia Travel Speed: 5 ipm Shielding Gas: He, 50 CFH Torch, 75 CFH Trailer, 10 CFH Backup			

Table 4 Weld Schedule C

Pass No.	V(v)	I(A)	Y-Wire Speed (ipm)	Ti-6Al-4V Wire Speed (ipm)
1	9.5	135	20.0	0
2	9.5	137	20.0	0
3	9.5	140	8.0	3.6
4	10.0	140	10.0	2.6
5	10.0	147	10.0	2.6
6	10.0	147	10.0	2.4
7	10.0	147	10.0	2.8
8	10.0	147	6.0	3.0
9	10.0	147	6.0	3.0
10	10.0	147	6.0	3.1
11	10.0	147	6.0	3.1
12	10.0	147	6.0	3.4
13	10.0	147	6.0	3.0
14	10.0	147	6.0	3.5
15	10.0	147	6.0	5.5
Base Metal: Ti-6Al-4V, 0.05 in. Thick Plate Filler Metal: Ti-6Al-4V-0.05Y, 0.045 in. dia Helium Shield Gas: 50 CFH Torch, 75 CFH Traller, 10 CFH Backup Torch Travel Speed, 5 ipm				

Table 5 Weld Schedule D

Pass No.	V(v)	I(A)	Y-Wire Speed (ipm)	Ti-6Al-4V Wire Speed (ipm)
1	8.5	140	25	0
2	9.0	135	25	0
3	8.0	160	20	3.8
4	8.5	165	20	3.5
5	8.5	165	20	3.8
6	8.5	165	20	4.2
7	9.0	165	18	5.7
8	9.0	170	18	7.0
9	9.0	173	18	6.8
10	9.0	173	18	7.5
11	9.5	180	16	8.5
12	9.5	180	16	8.6
13	9.5	190	16	8.9
14	9.5	193	16	8.2
15	9.5	200	15	10.6
16	9.5	200	16	10.8
17	9.5	200	16	12.1
18	9.5	200	15	9.8
19	9.5	200	16	9.1
20	10.0	200	16	8.9
Base Metal: Ti-6Al-4V, 0.875 in. Thick Plate Filler Metal: Ti-6Al-4V-0.5Y, 0.045 in. dia and Ti-6Al-4V, 0.125 in. x 0.125 in. Helium Shield Gas: 50 CFH Torch, 75 CFH Traller, 10 CFH Backup Travel Speed: 5 ipm				

Table 6 Weld Schedule E

Pass No.	V(v)	I(A)	Wire Speed (ipm)
1	8.5	140	20
2	7.4	140	25
3	8.7	152	35
4	8.7	150	36
5	8.7	168	36
6	8.7	180	36
7	8.7	180	36
8	8.7	185	40
9	8.7	187	40
10	9.0	190	45
11	9.0	195	45
12	9.0	195	45
13	9.0	195	45
14	9.0	195	45
15	9.0	195	45
16	9.0	195	45
17	9.0	200	45

Base Metal: Ti-6Al-4V, 0.875 in. Thick Plate
 Filler Metal: Ti-6Al-4V-0.5Y, 0.048 in. dia
 Helium Shield Gas: 50 CFH Torch, 75 CFH
 Trailer, 10 CFH Backup Gas
 Travel Speed, 5 ipm

Table 7 Weld Schedule F

V = 11.8
 I = 120 Amp
 Torch Speed - 5 ipm
 Filler Wire (Ti-6Al-4V) Speed - 23 ipm

Table 8 Weld Schedule G

V = 11.8 V
 I = 120 Amp
 Torch Speed = 5 ipm
 Filler Wire (Ti-6Al-4V-0.5Y) Speed - 23 ipm

The test specimens consisted of approximately 6.0 in. long x 3.0 in. wide Ti-6Al-4V plates in three different thicknesses of 0.875 in., 0.500 in. and 0.160 in. A 30° V-groove, as shown in Figure 2, was used for all 0.500 and 0.825 in. thick plates while 0.160 in. thick plates were "bead-on-plate" welds. To completely fill the V-groove in thicker specimens, a bead overlap technique, as illustrated in Figure 3, was used.

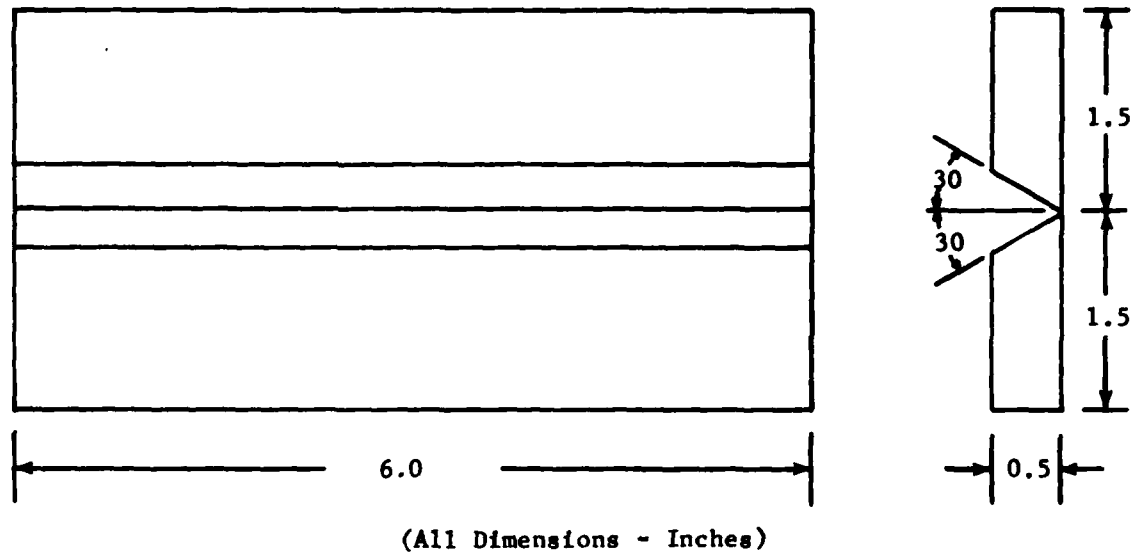


Figure 2 V-Groove Geometry

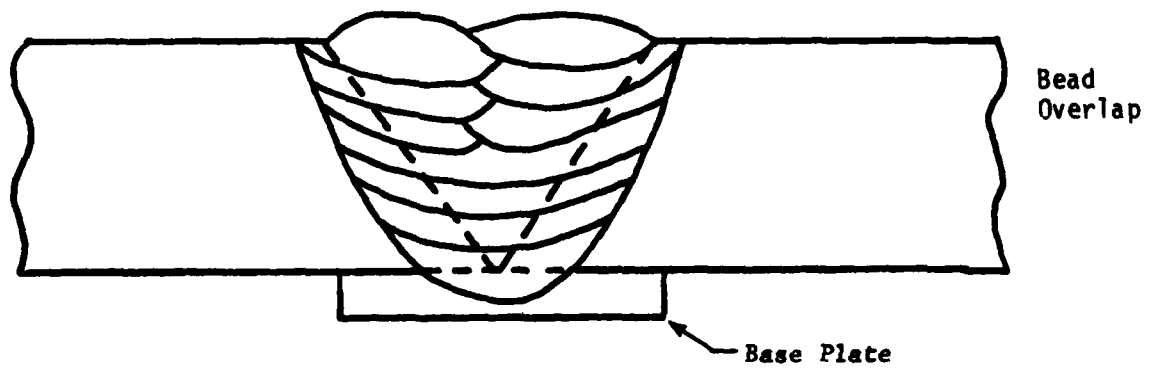


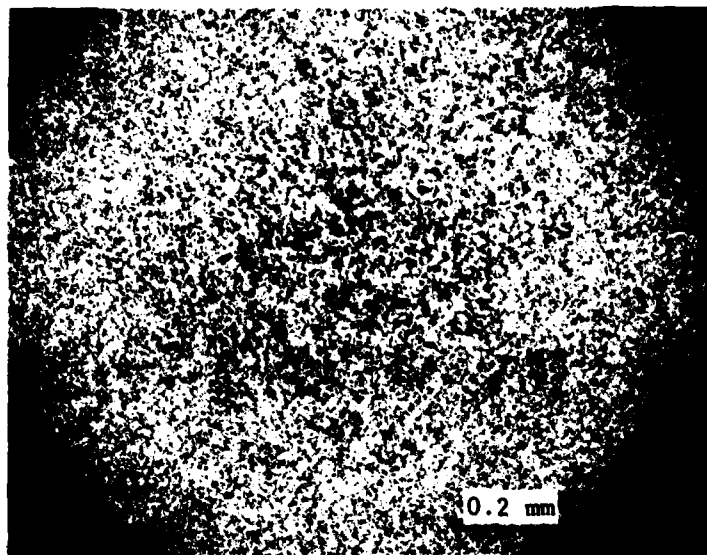
Figure 3 Bead Overlap Sequence in Multiple Pass Welds

Yttrium Filler Wire Fabrication

A Ti-6Al-4V ingot with approximately 0.5 wt % Y was vacuum cast in a water cooled tantalum crucible, with the approximate dimensions of 6.0 in. long and 3.0 in. dia. The cast ingot was machined to obtain smooth surfaces and preheated to 1725°F before extruding into 1.0 in. dia rods. The complete processing sequence was as follows:

- 1) Vacuum Cast (3.0 in. dia x 6.0 in. long);
- 2) Machining;
- 3) Preheat at 1725°F;
- 4) Extrude (1.0 in. dia);
- 5) Anneal at 1425°F for 2 h;
- 6) Hot swaged (0.650 in. dia);
- 7) Anneal at 1425°F for 2 h;
- 8) Warm swaged (0.300 in. dia);
- 9) Anneal at 1350°F for 3 h;
- 10) Cold drawn (0.110 in. dia);
- 11) Anneal at 1475°F for 7 h;
- 12) Cold drawn (0.048 in. dia);
- 13) Anneal at 1350°F for 2 h.

All the annealing operations were performed in vacuum. The final chemical composition of the wire was Al-6.17 wt %, V - 3.90 wt %, Y - 0.48 wt % and balance titanium. The microstructure of the wire, as shown in Figure 4, exhibited a very fine grain size and uniform distribution of yttrium containing particles.



0.048 in Diameter Ti-6Al-4V-0.5Y Wire

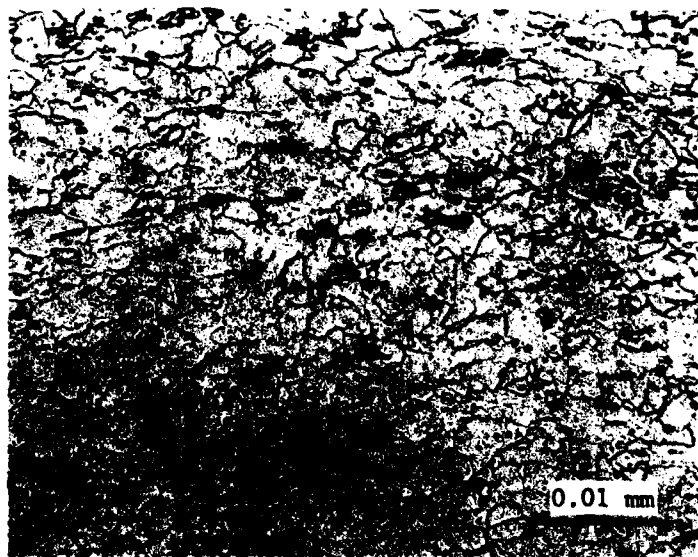


Figure 4
Microstructure of 0.048 in Diameter
Ti-6Al-4V-0.5Y Wire Showing Uniform
Y Distribution

RESULTS AND DISCUSSIONS

Effects of Heat Input - Figure 5 shows a transverse section of a 15 pass weld prepared according to weld schedule A. The extended columnar grains are clearly evident and appear to grow from the initial FZ/HAZ interface, then continue to grow across the fusion zones from bead to bead. Some grains are lost between adjoining beads because of the competitive growth process; however very few new grains seem to nucleate in the fusion zone. This particular weld was made with a heat input of approximately 15 kJ/in. (0.59 kJ/mm), which was kept constant for each pass. In the next iteration, weld schedule B, heat input was increased in each successive pass by increasing the weld current from 135 to 200 Amp. The resultant grain structure is still one of long columnar grains, as shown in Figure 6. It can be concluded that heat input, at least within the experimental range of 15 kJ/in. (0.59 kJ/mm) to 24 kJ/in. (0.94 kJ/mm), does not have a significant effect on the nucleation and growth phenomena which result in the coarse columnar grain structure previously described.



Figure 5
GTA 15 Pass Weld in Ti-6Al-4V, Ti-6Al-4V Filler
Wire, Constant Heat Input, Showing Long Columnar
Grain Structure

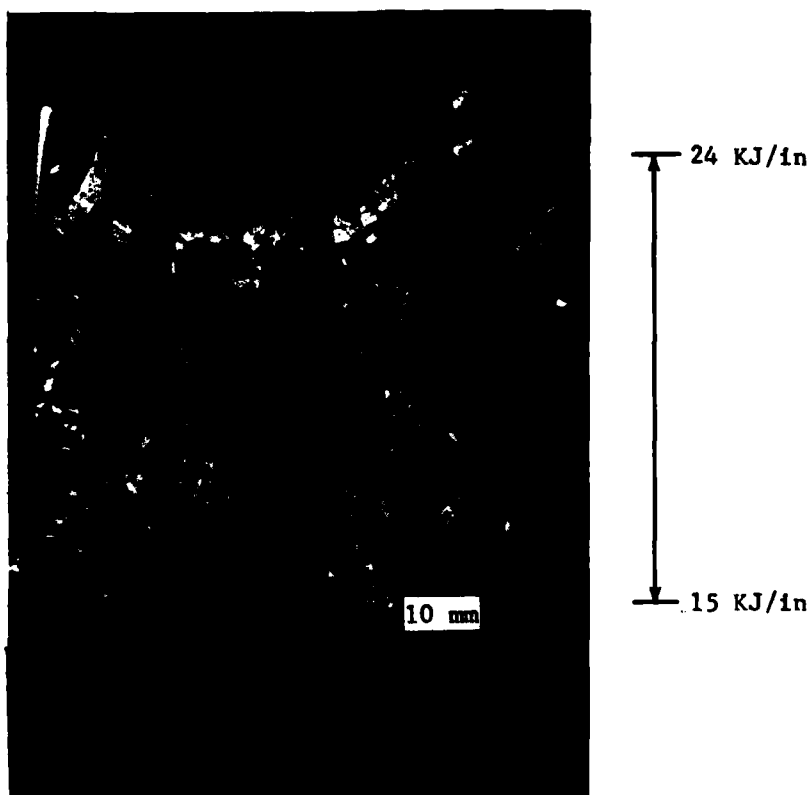


Figure 6
GTA Multipass Weld in Ti-6Al-4V with
Ti-6Al-4V Filler Wire

Effects of Yttrium Additions - The effects of yttrium microalloying was studied by preparing several welds with the process variables as shown in Table I. All yttrium modified welds exhibit significant grain refinement. The transverse section of a 20 pass weld (schedule D) is shown in Figure 7. The cracking of the plate occurred after the last pass which was made at a high input of 24 kJ/in., however it clearly establishes the breakdown of long columnar grains. A longitudinal section of another weld prepared according to weld schedule E is shown in Figure 8 along with the yttrium concentration profile. This weld was selected for detailed microstructure studies. The area marked 'A' in Figure 8 does not contain any yttrium and the grains grow across the total fusion zone similar to welds shown in Figures 1 and 6. A higher magnification view of this area (Figure 9) shows the grains growing epitaxially across the fusion line, as expected. The area marked B in Figure 8 contains 0.04% yttrium and shows equiaxed grains in the fusion

zone, as shown in Figure 10, however grains still grow epitaxially from the previous FZ/HAZ interface even though many yttrium compound particles are observed to be uniformly distributed at this interface (Figure 11). It could be concluded from this observation that yttrium does not interfere with the epitaxial growth at the FZ/HAZ interface. A transition from equiaxed to long columnar grain structure as a function of Y modification is shown in Figure 12.

Another significant observation is that the grain refinement in the fusion zone occurs some distance away from the FZ/HAZ interface as shown in Figure 12. The phenomenon is more clearly demonstrated in a single pass weld containing 0.1% yttrium as shown in Figure 13. The initial long grains grow epitaxially, followed by equiaxed grains in the center of the pool. This observation is similar to that found by Simpson¹⁰ in Ti-6Al-6V-2Sn welds. He proposed that concentration of yttrium compound particles builds up at the advancing solid-liquid front and the resulting drag effect may induce the undercooling required for nucleation. Simpson's theory was based on the experimental observation that yttrium precipitates were concentrated at the grain boundaries, and that the concentration increased as the solidification progressed. However, in this study, a uniform distribution of yttrium particles, rather than particles segregated at grain boundaries, was observed, as shown in Figure 14, indicating that some other mechanism might be operative.

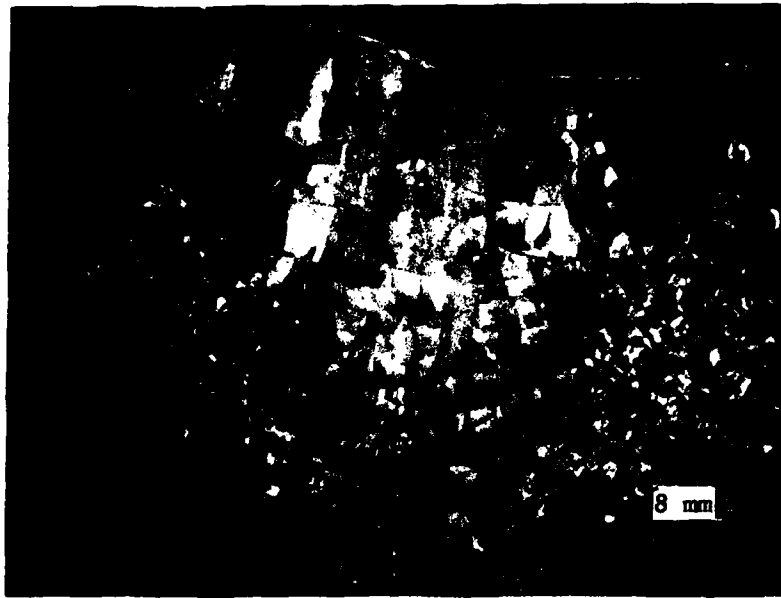


Figure 7
Y-Modified 20-Pass Weld (Schedule D) Showing Fine
Grains Compared to Columnar Grains for No Y Welds
Shown in Figure 6

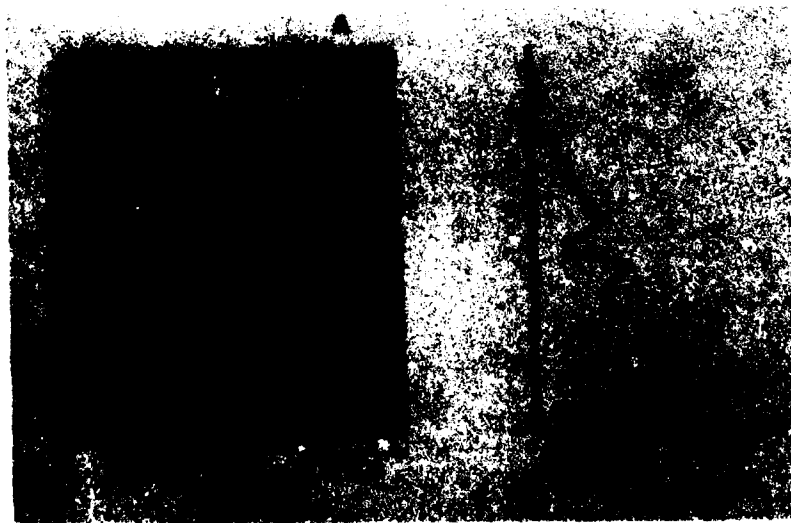


Figure 8
GTA 20 Pass Weld in Ti-6Al-4V with Varying Heat Input and
Yttrium Concentration (Parallel to the Weld Direction)

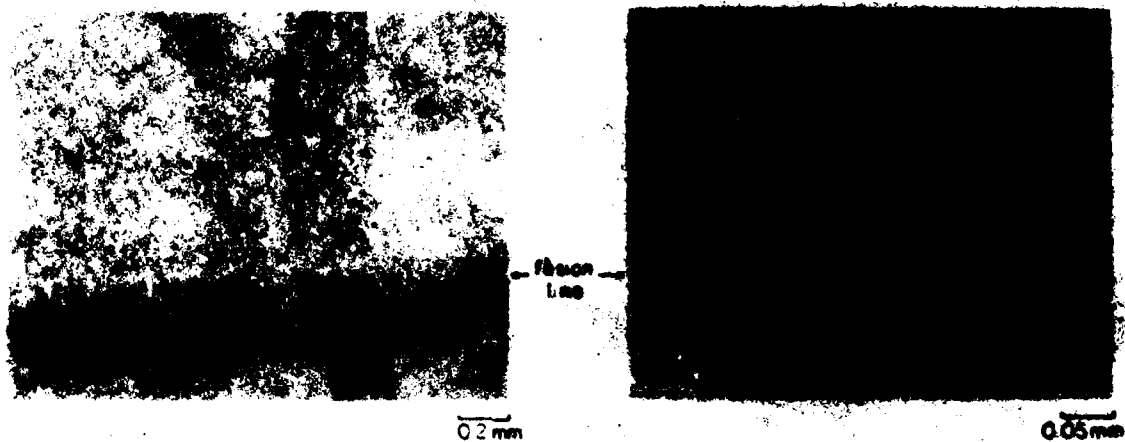


Figure 9
Area A - Epitaxial Grain Growth across the Fusion Line (Kroll's Agent)



Figure 10
Area B - Equiaxed Grains between Two Fusion Lines

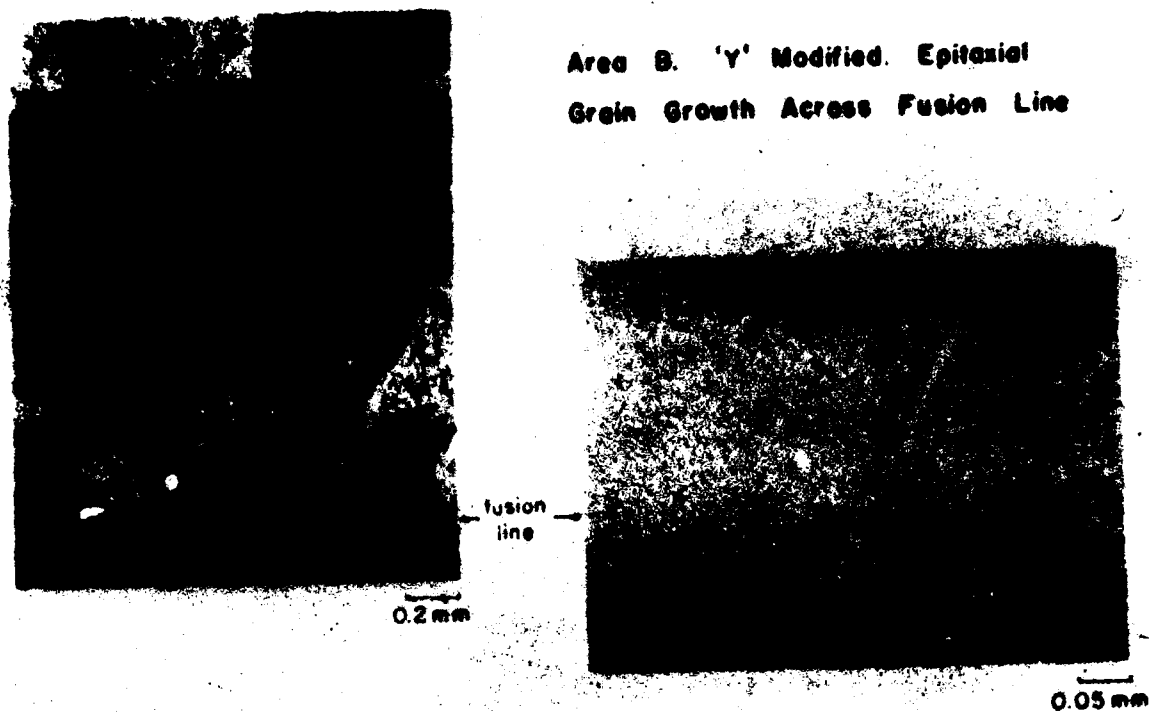


Figure 11
Area B - Epitaxial Grain Growth across Fusion Line. Uniform Distribution of Yttrium Inter-Metallic Compounds are Clearly Visible at the Interface.

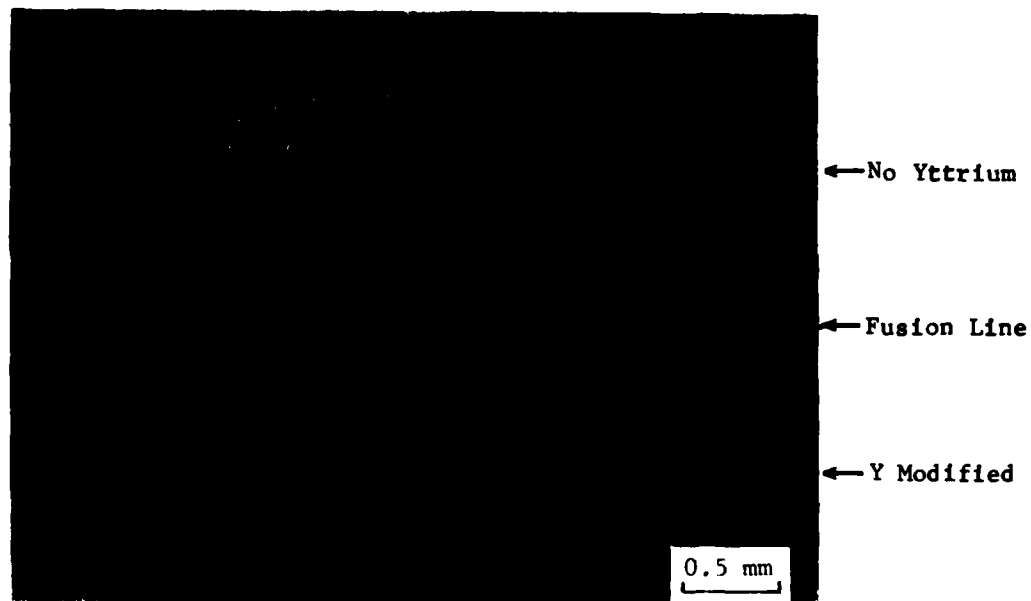


Figure 12
Transition in Grain Structure from Y-Modified to No-Y Weld
Passes Near Area A in Figure 8

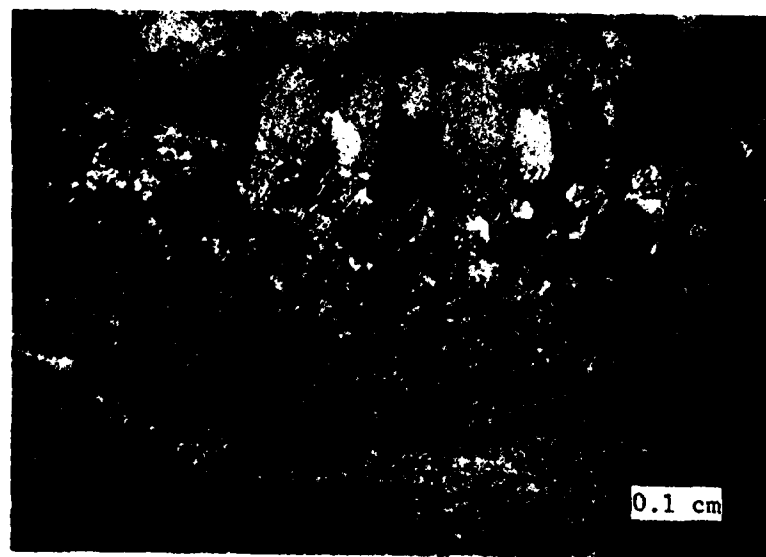


Figure 13
Bead-on-Plate Weld Showing Epitaxially Grown
Columnar Grains at FZ/HAZ Interface Followed By
Equiaxed Fine Grains



*Figure 14
Area B - Equiaxed Grains with Uniform Yttrium Inter-Metallic Compound
Distribution; Note Absence of Any Grain Boundary Segregation (Kroll's
Agent)*

Transmission Electron Microscopy

Figure 15 shows the structure of the base metal which was a rolled plate in the annealed condition. The structure consists of primary equiaxed α and acicular α in transformed β . The fusion zone microstructure is primarily martensitic α' . The transmission electron micrograph also shows α -phase laths separated by thin strips of β -phase and probably an interface layer structure at the α/β interface, as shown in Figure 16.

The objective of the TEM study was to characterize Y particle morphology and understand their role in nucleation and growth phenomenon. It is shown in Figure 17 that Y containing particles are distributed in the α' matrix. The particles have two distinct morphologies, one plate-like or cuboid (Fig. 18) and other dendritic, as shown in Figure 19. In many instances both types overlap or are in close proximities.

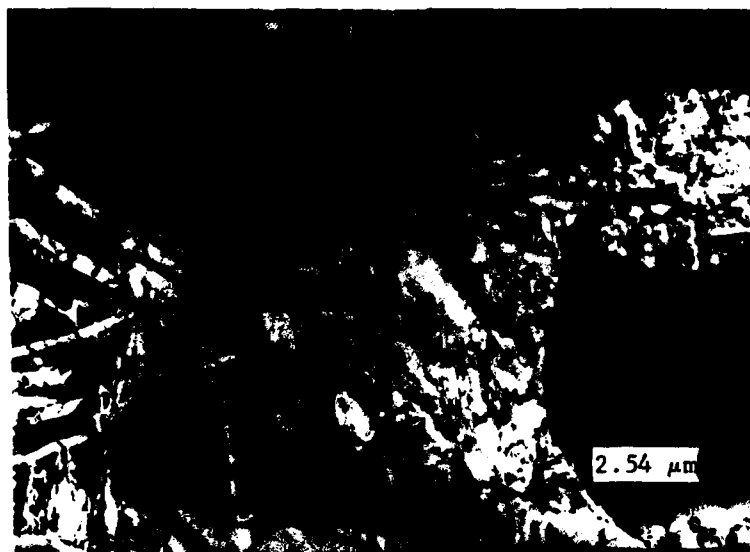


Figure 15
Transmission Electron Micrograph of the Base Metal
Showing Equiaxed Primary α and Acicular α in the
Transformed β Matrix



Figure 16
Transmission Electron Micrograph of Y-Modified
Fusion Zone Showing Alternate Layers of α (Light)
Separated By Thin Strips of β -Phase

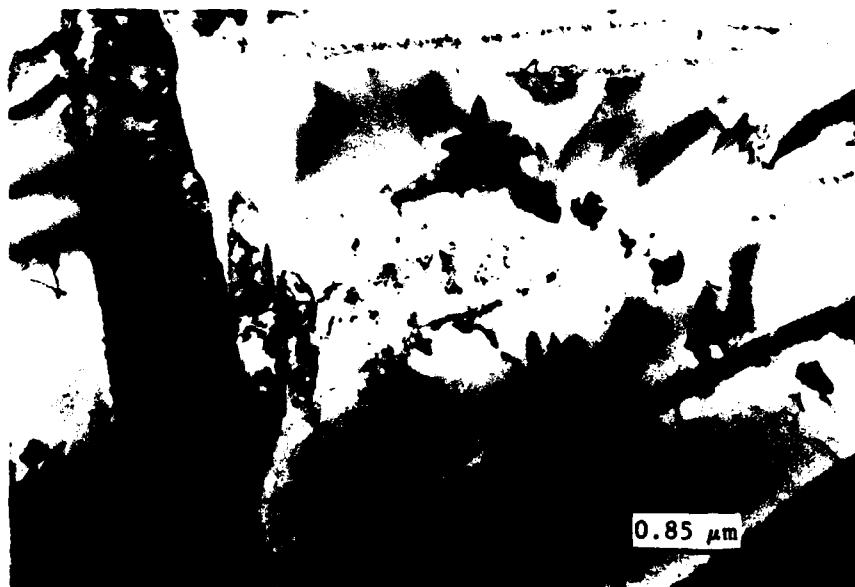


Figure 17
Transmission Electron Micrograph of Y-Modified
Fusion Zone Showing Y Particle Distribution in
 α' Matrix

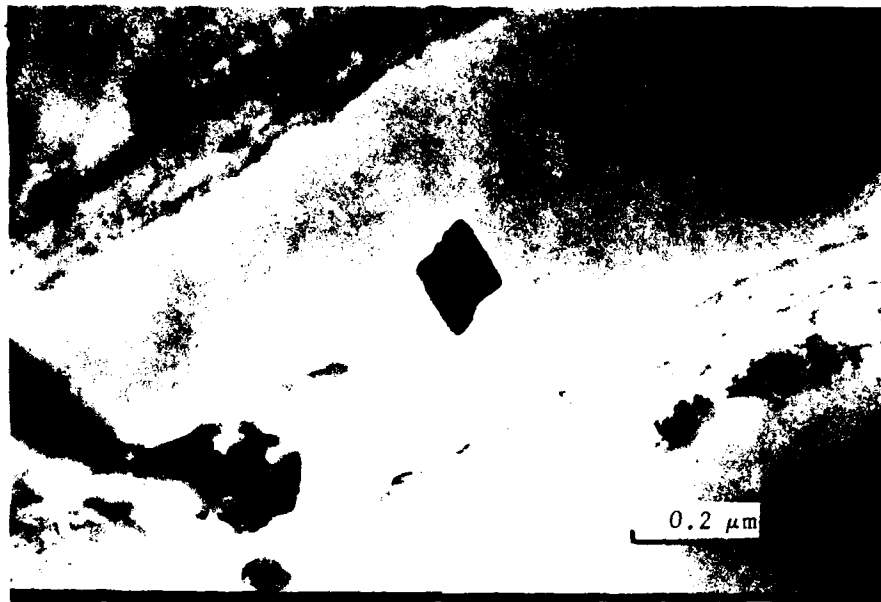


Figure 18
Transmission Electron Micrograph, Same As Figure
17, Showing Plate Like Morphology of Y Particles

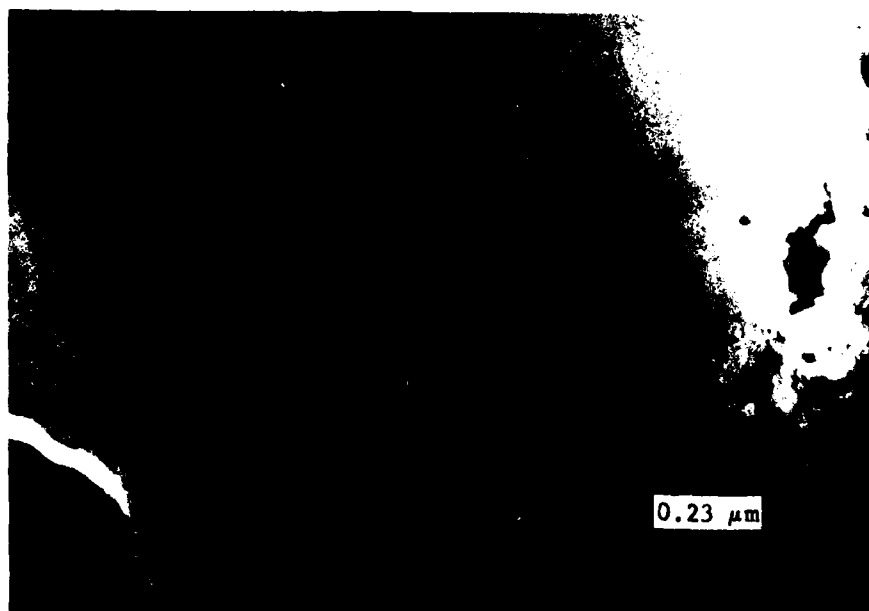
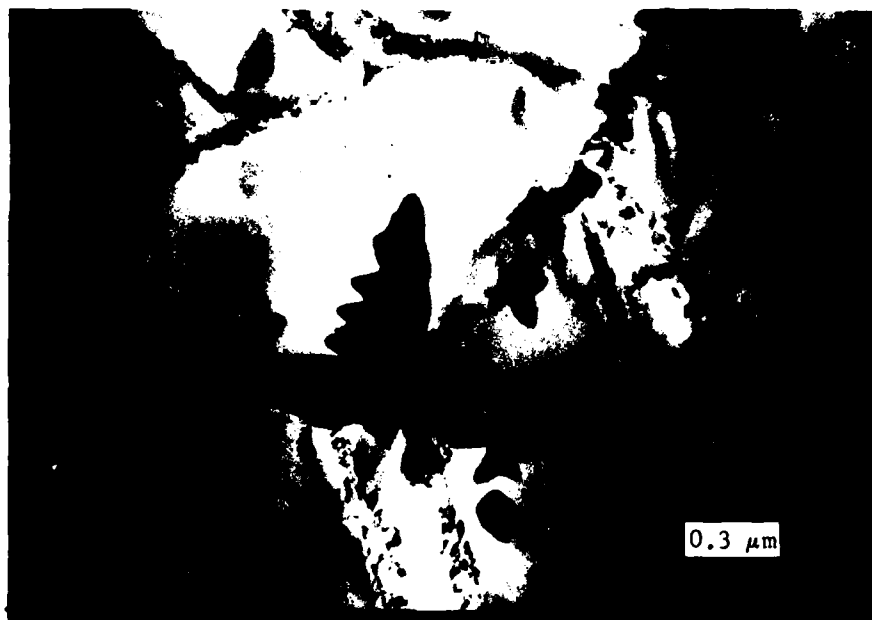


Figure 19
Transmission Electron Micrograph, Same As Figure 17,
Showing Dendritic Morphology of Y Particles

It was extremely difficult to establish the chemical nature of these particles, however, they were speculated to be Y_2O_3 based on the results of X-Ray Electron Spectroscopy (XES) and backscatter electron analysis, presented in Figure 20 through 23.

The dendrites are grown from the melt during the weld pool solidification, where Y combines with oxygen present in the melt. The cuboids are probably inclusions when Y was oxidized to Y_2O_3 before entering the weld pool, consequently it never formed a part of the melt.

Both the particles are randomly distributed with no preferential segregation sites. It is not clear from this limited work which one of the particles is responsible for the observed grain refinement.

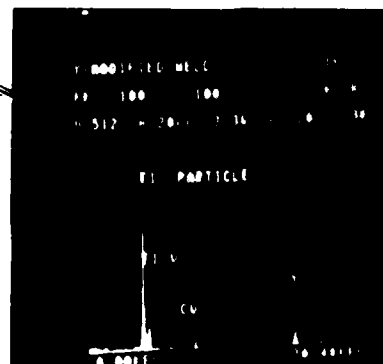
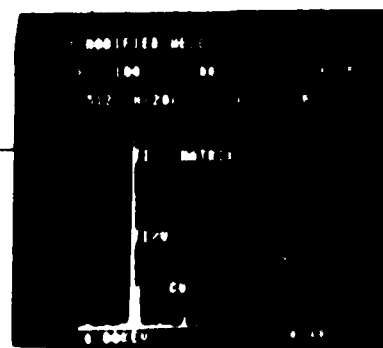


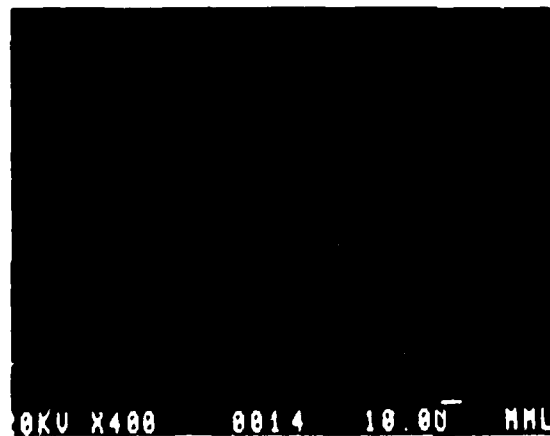
Figure 20
XES Analysis of the Particles and the Matrix in
Y-Modified Fusion Zone



Figure 21 Yttrium Scan of a Dendritic Particle

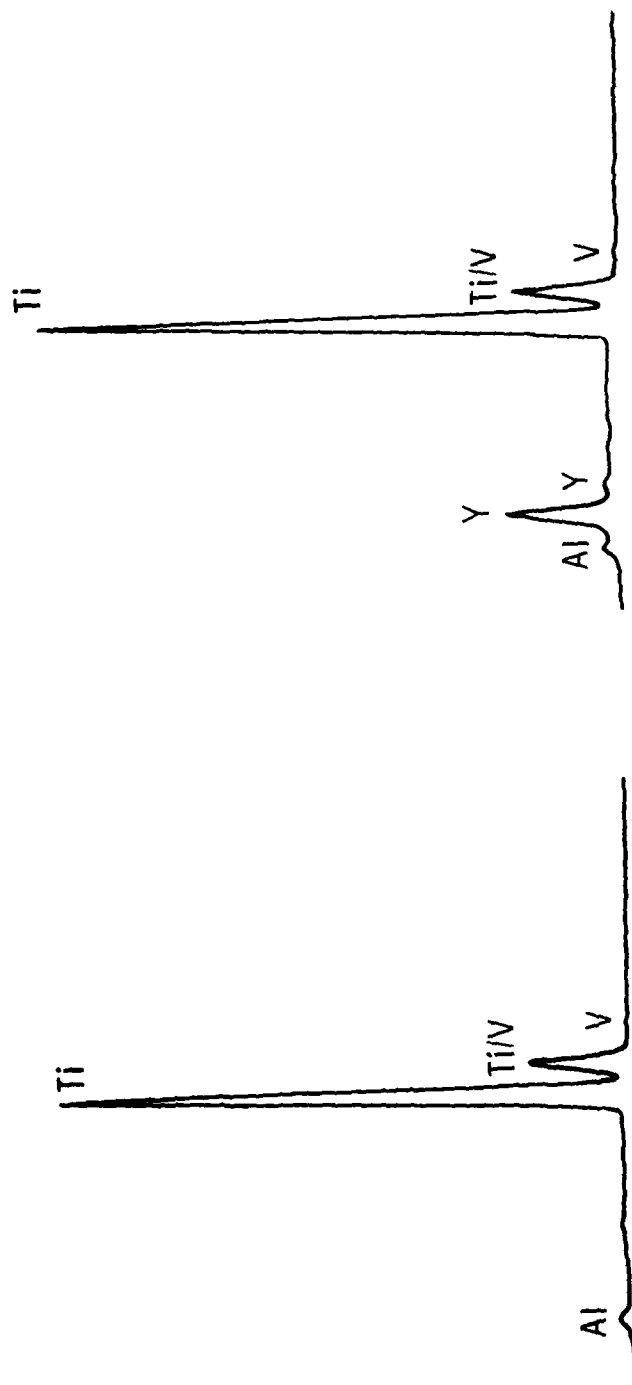


Parent Metal



Weld

*Figure 22
Backscattered Electron Images of Y-Modified
Welds Showing Uniform Distribution
of Y-Containing Particles*



Matrix Analysis in Y - Modified Ti Weldment Particle Analysis in Y - Modified Ti Weldment

Figure 23
XES Analysis Results of Fusion Zone Matrix and the Particles

Basic Model for Grain Refinement

The experimental observation that grain refinement occurs away from the FZ/HAZ interface in the presence of yttrium, suggests that the refinement is controlled by some type of time dependent processes such as nucleation and/or growth. Therefore the fundamental theories of nucleation and growth were applied to develop a model to explain the refinement mechanism.

The classical heterogeneous nucleation and growth theories¹² relate the structure of a material solidification from the melt to supercooling and surface tension effects. The nucleation rate is given as:

$$[1] \quad I = c_1 \exp - \frac{16\pi\sigma^3 T_m^2 V_s^2}{3\Delta H^2 (\Delta T)^2 kT} f(\theta)$$

where:

- I = rate of heterogeneous nucleation per unit volume of liquid;
- c_1 = constant;
- ΔH = heat of fusion;
- σ = liquid-solid interfacial energy;
- ΔT = degree of supercooling;
- T_m = melting temperature;
- k = Boltzman's constant;
- V_s = volume of solid;
- $f(\theta)$ = function of contact angle.

For a specific metal system, equation (1) can be rewritten as:

$$[2] \quad I = c_1 \exp - \frac{c_1'}{(\Delta T)^2}$$

The growth rate, R, is expressed as:

$$[3] \quad R = k(\Delta T)^n$$

where K and n are constants. The value of n is normally between 1 and 2; however, in this analysis, n is taken as 1, since the value of n does not affect the concept presented here. Similarly, ΔT for nucleation and ΔT for growth will be slightly different for each other however, they are directly related and can be equated through a constant.

The above relationships can be applied to weld pool solidification by introducing the concept of two competing times:

- 1) t_n = time to nucleate one grain;
- 2) t_g = time for one grain to grow across the bead.

During the solidification of any given weld pass, if $t_n > t_g$, then the grain will grow completely across the bead before any other grain is nucleated. This situation is evident in the microstructure seen in Figures 1, 5, 6, and 9 (Area A). But if $t_n < t_g$, then the epitaxially growing grain may impinge upon a newly nucleated grain, as shown schematically in Figure 24. This situation is similar to that observed in welds fabricated with yttrium-bearing filler wire, as shown in Figures 10 and 11.

Expressions for t_n and t_g can be obtained from equations (2) and (3). Differentiating equation (2) yields:

$$d \frac{n}{v} / dt = c_1 \exp \left[- \frac{c_1'}{(\Delta T)^2} \right]$$

$$\frac{dn}{dt} = c_1 v \exp \left[- \frac{c_1'}{(\Delta T)^2} \right]$$

This form of the equation can be integrated to express the time required to form a single nucleus, t_n :

$$\int_0^{n=1} dn = \int_0^{t_n} c_1 v \exp \left[-\frac{c_1'}{(\Delta T)^2} \right] dt$$

$$1 = c_1 v \exp \left[-\frac{c_1'}{(\Delta T)^2} \right] t_n$$

or

$$[4] \quad t_n = \frac{\exp \left[+\frac{c_1'}{(\Delta T)^2} \right]}{c_1 v}$$

Similarly, to calculate t_g , let us assume that the bead depth is x_o , as shown in Figure 25, then

$$R = \frac{dx}{dt} = K\Delta T$$

or

$$\int_0^{x_o} dx = \int_0^{t_g} K\Delta T dt$$

$$x_o = K\Delta T t_g$$

or

$$[5] \quad t_g = \frac{x_o}{K\Delta T}$$

Equations 4 and 5 provide the relationship between t_g , t_n , and ΔT , which can be graphically represented in Figure 26.

Whether the weld pool solidification is growth controlled or nucleation controlled will depend upon two values of ΔT : ΔT_c - the critical amount of supercooling after which nucleation can occur rapidly and ΔT_w - amount of supercooling associated with the welding process as defined in Figure 27. If $\Delta T_w < \Delta T_c$, as shown in Figure 26, then the fusion zone grain structure will be long columnar, since $t_g < t_n$. However, if $\Delta T_w > \Delta T_c$ then new grains may nucleate since $t_g > t_n$.

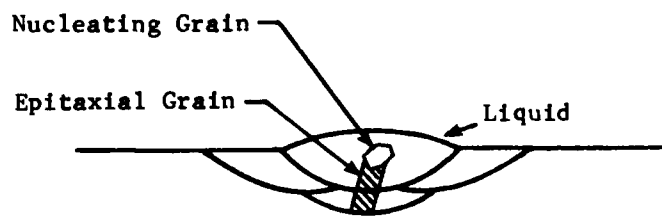
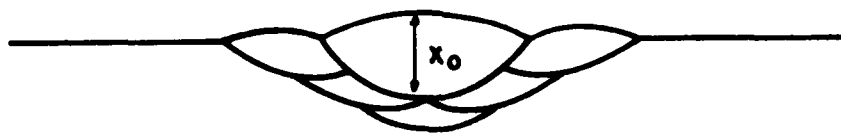
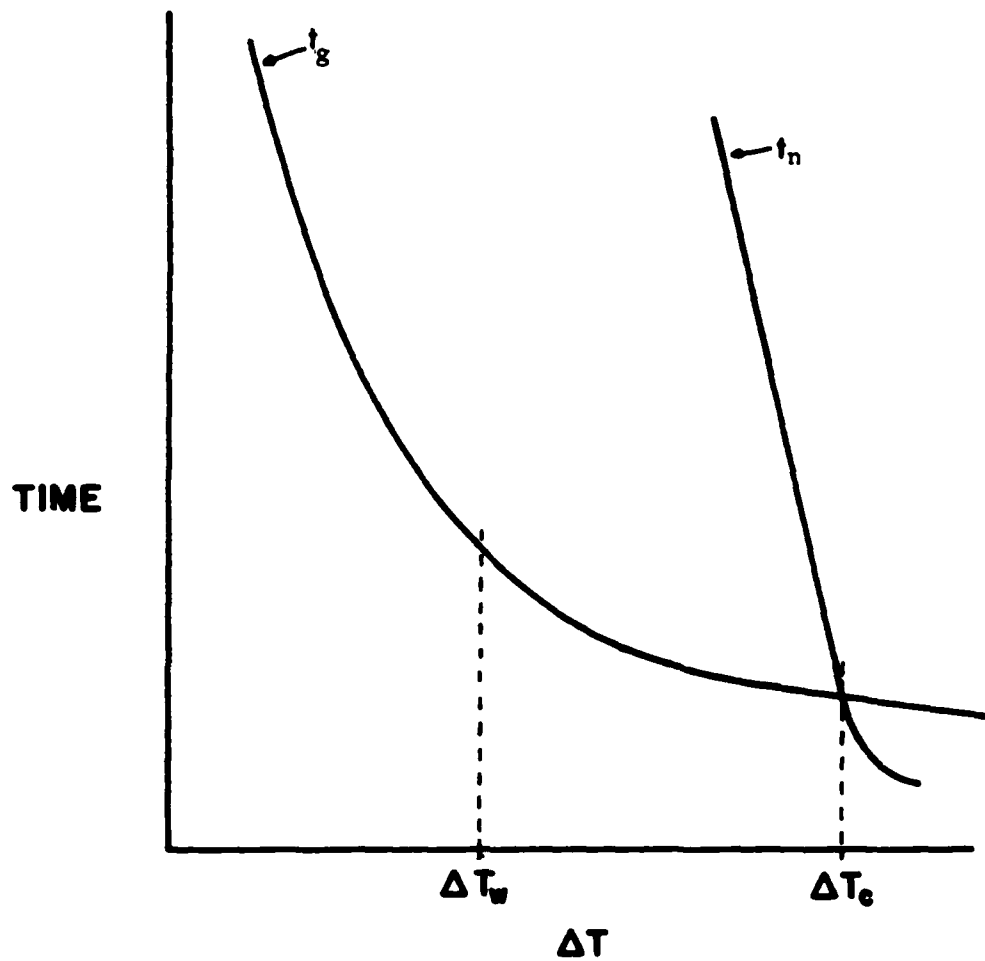


Figure 24
A Schematic Presentation of an Epitaxially Growing Grain Being Stopped by a New Nucleating Grain



x_0 = distance across bead

Figure 25 Definition of Bead Depth, x_0



t_g - time to grow across the bead
 t_n - nucleation of one grain

Figure 26
Nucleation and Growth Time vs Supercooling in Weld Pool
Solidification

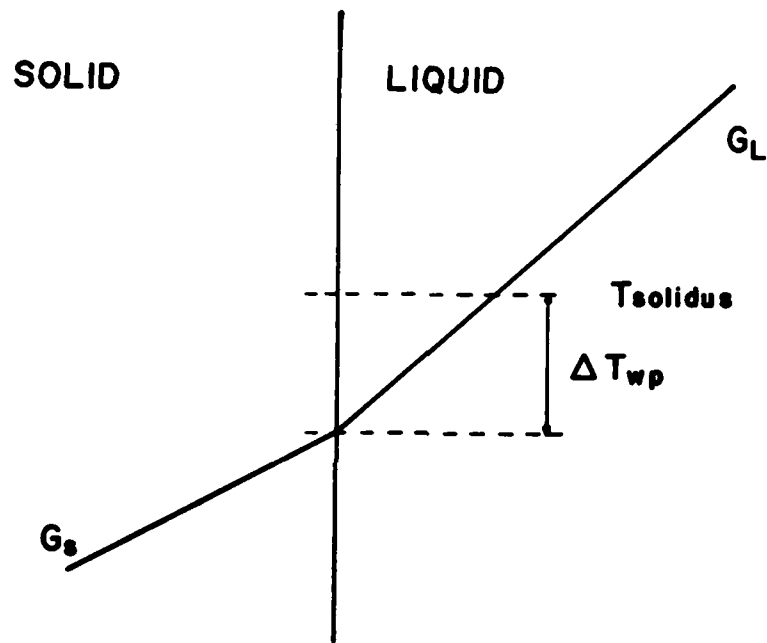
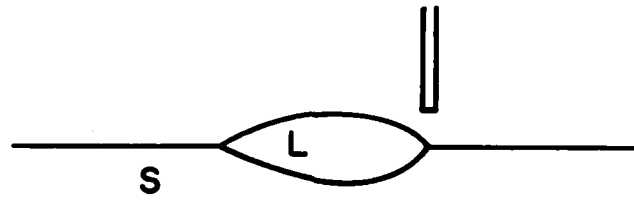


Figure 27 ΔT Associated with the Welding Process

Minor alloying elements are known to reduce ΔT_c required for heterogeneous nucleation. If the ΔT_c and nucleation curve in Figure 26 can be shifted towards the left hand side past the ΔT_w , then new grains may nucleate before epitaxial grains can grow across the total fusion zone. This reduction in ΔT_c and the shift in the nucleation curve can be fundamentally interpreted as a change in the liquid-solid interfacial energy, σ , or contact angle, $f(\theta)$, due to the presence of yttrium, either in solution or as a yttrium-bearing particle. This concept will explain the observation that initial epitaxial growth is followed by equiaxed grains in Ti-6Al-4V welds fabricated with yttrium-bearing wire.

Experimental Verification of the Basic Model

The critical question concerns the mechanism responsible for the observed grain refinement caused by yttrium additions. Does yttrium act as a nucleating agent by providing more sites for heterogeneous nucleation, or does it retard the grain growth kinetics? It is entirely possible that yttrium affects surface tension and the fluid motion of the weld pool to refine the structure by the grain multiplication technique similar to that observed in castings. As a matter of fact, the weld pool fluid flow was observed to be more turbulent in the presence of yttrium. In this study, however, efforts were directed towards understanding of nucleation and growth kinetics and not towards surface tension driven fluid flow.

To verify the basic model, growth velocity and nucleation time were determined experimentally as described below.

Growth rate of the solidification front: A longitudinal section of a Ti-6Al-4V weld prepared with Ti-6Al-4V filler is shown in Figure 28. It shows the grain direction almost 90° from the welding direction. A similar weld section (Figure 29) prepared with yttrium modified filler wire shows the different grain orientation. Grains are growing in the direction of the moving solidification front in the weld pool. The growth rate of the solidification front, R , can be determined by a simple vectorial approach from the knowledge of the welding torch travel

speed, V , and angle θ , between the columnar grains and the welding direction from the relationship,

$$R = V \cos \theta$$

A pictorial relationship between R , V and θ is shown in Figure 30. The angle θ is definitely influenced by the yttrium additions as can be seen in Figure 31, which is a longitudinal section of a 22 pass Ti-6Al-4V weld with varying yttrium concentrations in each pass. (In contrast, a weld made with no Y filler addition shows nearly perpendicular columnar grains as seen in Figure 32). The grain orientation changes with Y concentration, increasing Y decreases the angle θ as shown in Figure 33. The growth rate (R) for this case as a function of Y concentration was calculated using equation 6 and the results are presented in Figure 34. It is apparent that yttrium additions increased the growth rate.

Nucleation Time - With the knowledge of the growth rate, the time to nucleate the first grain in the weld pool (t_n) can be calculated by measuring the distance along the epitaxially grown grains to the first equiaxed grain (l_1) as shown in Figure 35 and applying a linear growth equation:

$$l_1 = R t_n$$

The nucleation time for 0.1 wt% yttrium addition was calculated and is presented in Table 9. The time to nucleate the first grain in the weld pool was found to decrease by more than an order of magnitude, from 13.9 s to 0.48 s.

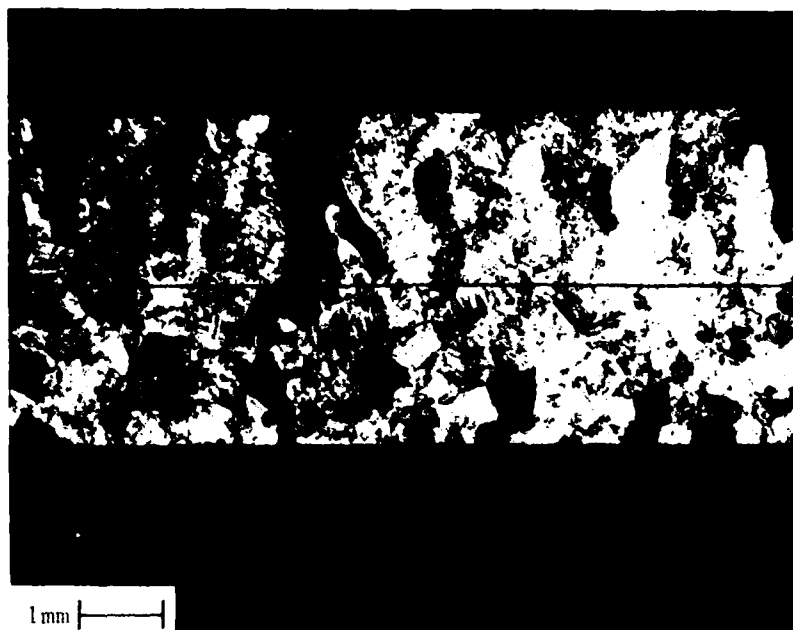


Figure 28
Single-Pass Weld (Schedule F) with Ti-6Al-4V Filler
Wire Showing Grain Orientation

Welding Direction →

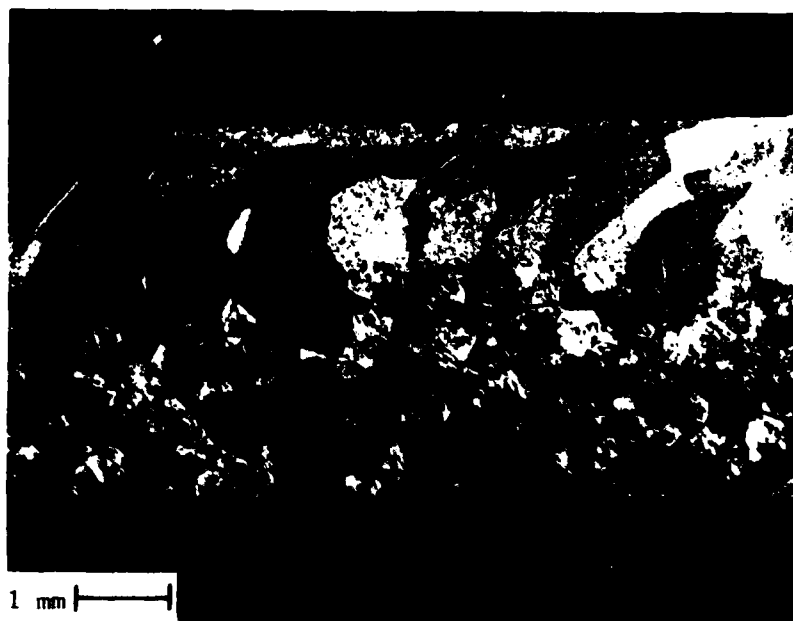
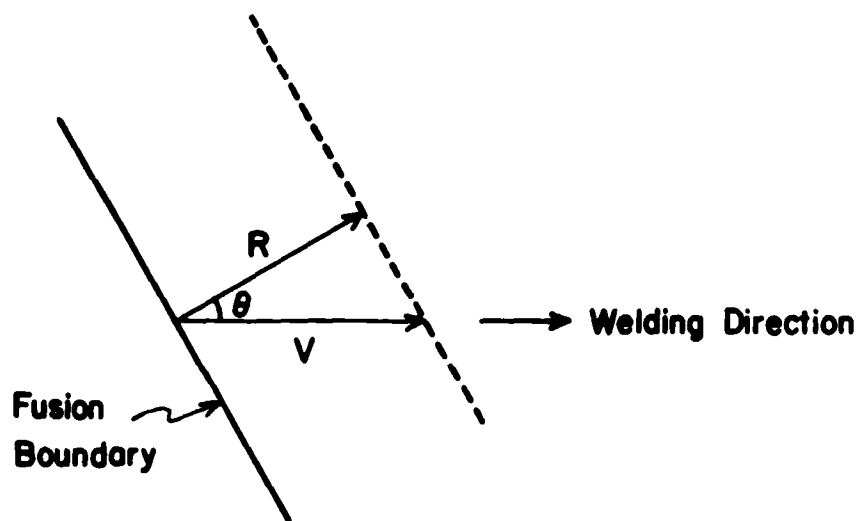


Figure 29
Single-Pass Weld (Schedule G) Prepared with Y-Modified
Filler Wire Showing Grain Orientation



$$R = V \cos \theta$$

R - Growth Rate

V - Arc Speed

Figure 30
Vector Approach to Determine Velocity of Solidification
Front

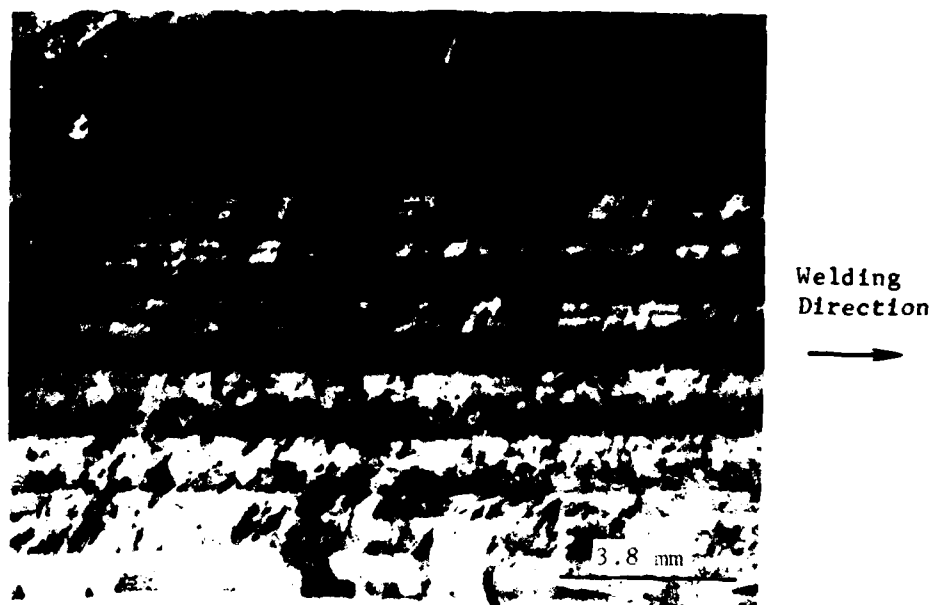


Figure 31
*Multiple-Pass Weld (Schedule E) with Varying Y Concentration;
 Grain Orientation with Respect to Welding Direction Changes
 As a Function of Y Concentration*

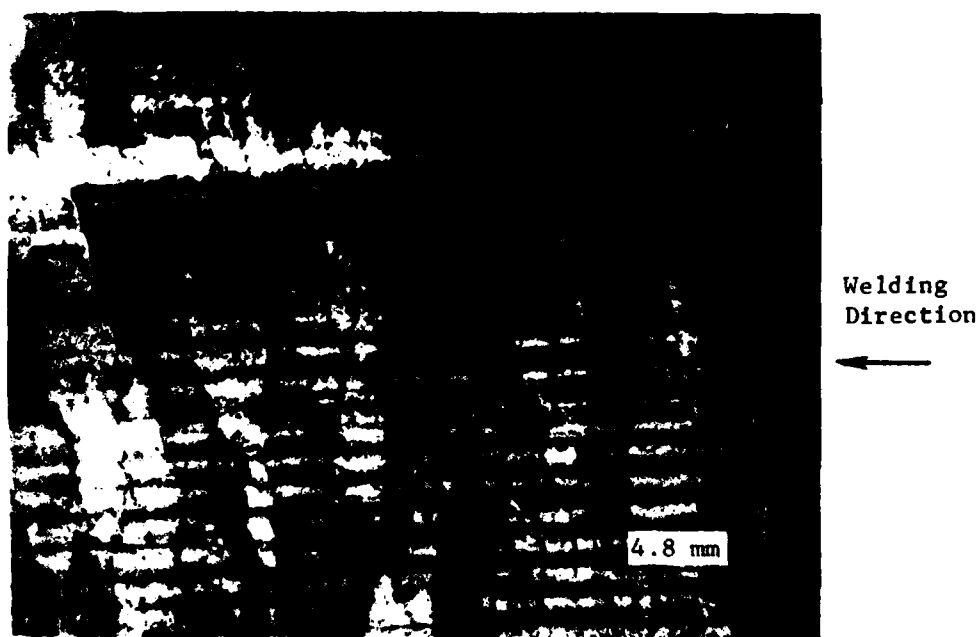


Figure 32
*Multiple-Pass Weld (Schedule B) Showing Columnar
 Grains Almost Perpendicular to Welding Direction*

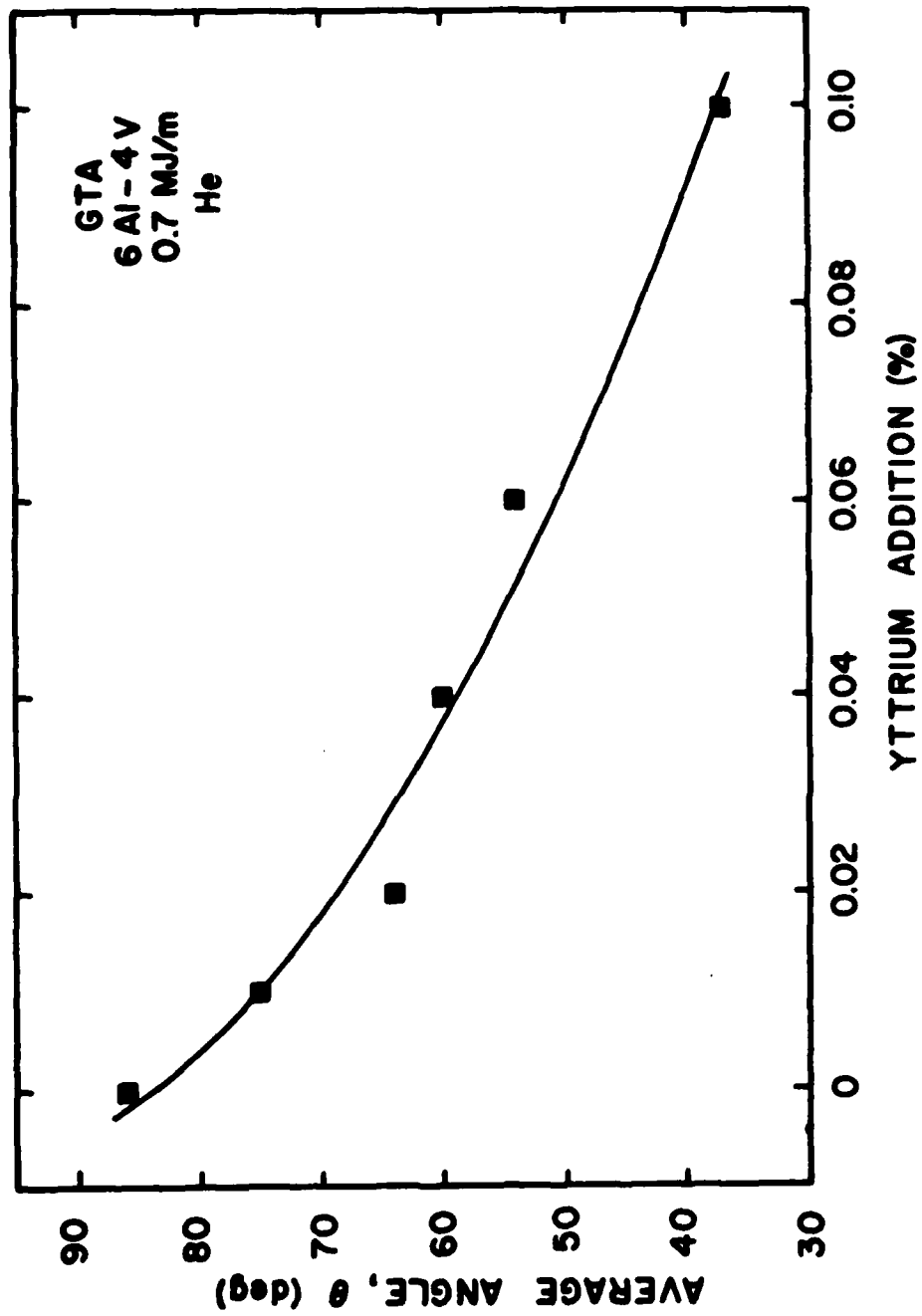


Figure 33 Change in Grain Orientation as a Function of Y Addition

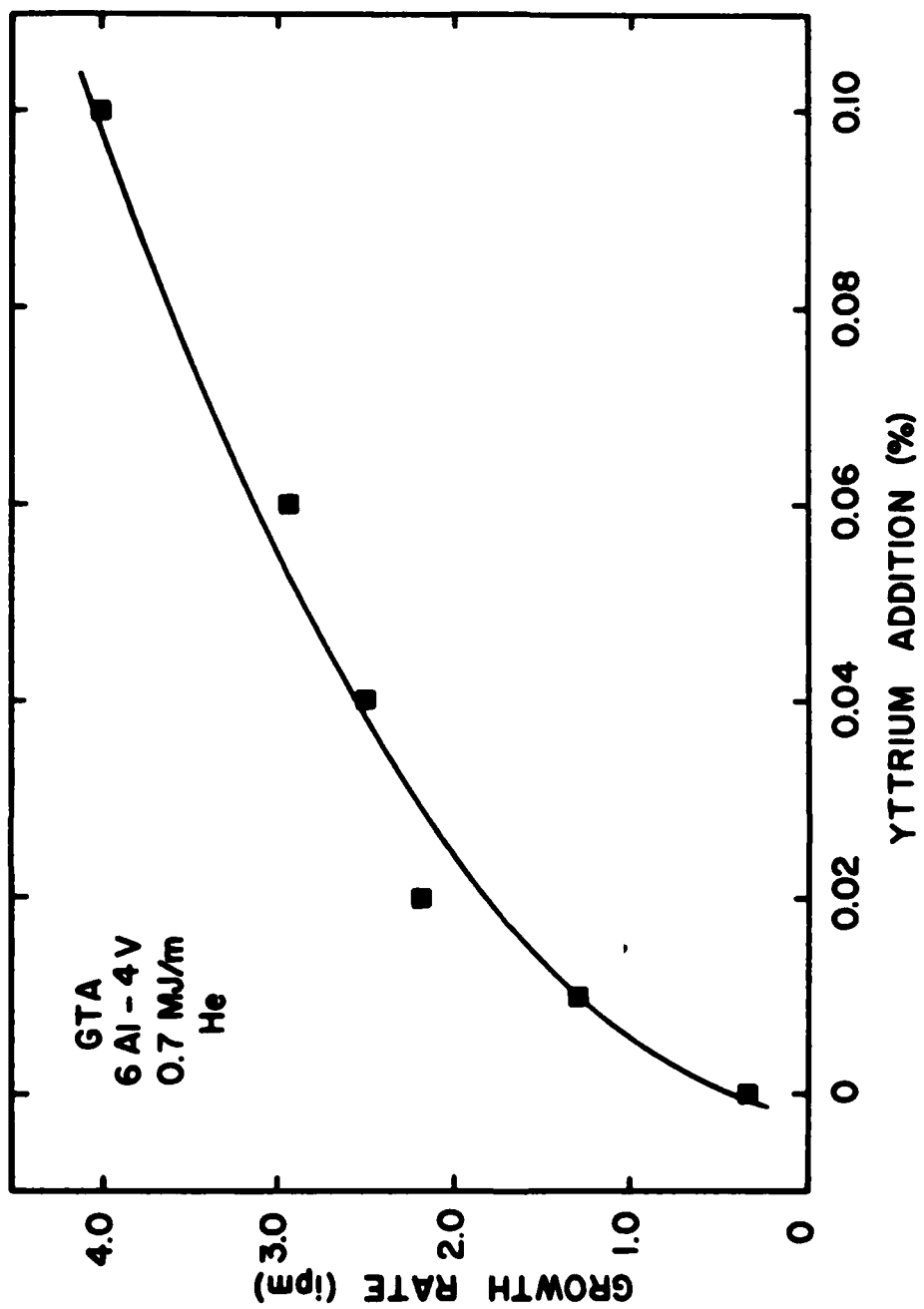
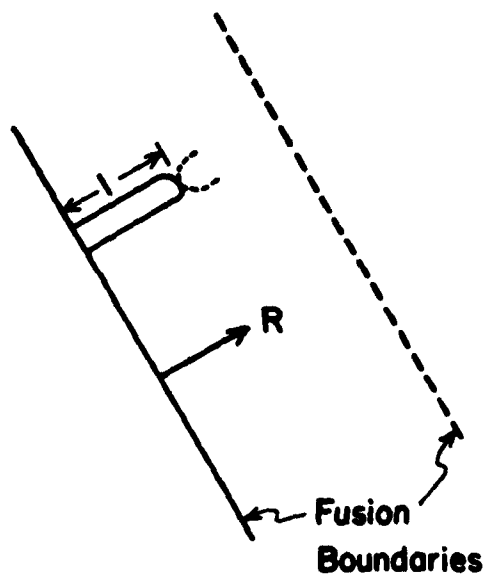


Figure 34 Effect of Y Addition on the Rate of Solidification Front Movement



$$l = Rt$$

$$t = \frac{l}{R}$$

t_i = time to nucleate one grain

Figure 35
Determination of Nucleation Time (t_n)

Table 9
Effect of Y Addition on
Solidification Kinetics

%Y	R (ipm)	I (in.)	t_n (sec)
0.0	0.34	0.08	13.9
0.1	3.99	0.03	0.48

It is very apparent that grain refinement in Ti-6Al-4V welds by microalloying with Yttrium is controlled by the competition between the nucleation and growth processes. Yttrium increases the rate of solidification front movement from 0.34 ipm to 3.99 ipm for 0.1 wt % Y, which should favor the long columnar grains. Concurrently however, Y addition also drastically decreases the time to nucleate the first grain in the fusion zone which results in grain refinement. Therefore for a given ΔT_w , if the reduction in nucleation time by Y microalloying outweighs the faster solidification front movement, the resultant fusion zone microstructure will be fine and equiaxed.

CONCLUSIONS

- Small additions of yttrium in the fusion zone of Ti-6Al-4V alloys significantly affects the solidification kinetics of the weld pool.
- Yttrium does not interfere with the epitaxial growth at the FZ/HAZ interface. Refinement is observed away from this interface, indicating some time-dependent process is the responsible mechanism.
- Grain refinement in the weld pool by microalloying can be explained by introducing two competing time concepts to the classical nucleation and growth theories developed for casting solidification.
- Both nucleation time and the solidification front motion in the weld pool can be very simply determined by microstructural observation of grain orientation and the dimension of the epitaxially grown grain.
- Yttrium increases the rate of solidification front movement which should favor the long columnar grains. Concurrently, however, it also decreases the time to nucleate the first grain which is a predominant factor responsible for the observed fusion zone grain refinement.
- Two different Y particle morphologies were observed: (1) plate-like; and (2) dendritic. It is not clear that either one or both of these particles provide grain refinement.

REFERENCES

1. C. R. Loper, Jr., L. A. Shidler, and J. H. Devletian: *Welding Journal*; Vol., 48, 171-S, April 1969.
2. W. F. Savage, C. D. Lundin, and A. H. Aronson: *Welding Journal*, Vol. 44, 175-S, April 1965.
3. Unpublished work, Advanced Manufacturing Technology Group. Martin Marietta Aerospace, Denver, Colorado.
4. D. C. Brown, F. A. Crosseley, J. F. Rudy, and H. Swartzbart: *Welding Journal*, Vol. 41, 241-S, June 1962.
5. W. F. Savage and A. H. Aronson, *Welding Journal*, Vol 45, 85-S, February 1966.
6. G. K. Turnbull, D. M. Patton, G. W. Form and J. F. Wallace: *Trans. Am. Foundrymen's Soc.*, Vol 69, p 792, 1962.
7. B. L. Bramfitt, *Met. Trans.*, Vol 1, p 1987, July 1970.
8. S. S. Glickenstein and W. Yeniscavich: *Welding Research Council Bulletin* 226, May 1977.
9. B. B. Rath, B. A. MacDonald, S. M. L. Sastry, R. J. Lederich, J. E. O'Neal, and C. R. Whitsett: *Titanium '80 Science and Technology*, Vol 2, p 1185.
10. R. P. Simpson: *Welding Journal*, Vol 56, 67-S, March 1977.
11. G. R. Edwards, D. R. Olson and D. K. Matlock: *Proceedings of T1-6211 Basic Research Program, DTNSRDC-SME-CR-15-82*, p 345, July 1982.
12. M. C. Flemings: *Solidification Processing*, McGraw Hill, New York, NY, 1974